Interface excitons in staggered-line-up quantum wells: The AlAs/GaAs case

R. Zimmermann
Max-Planck-Arbeitsgruppe "Halbleitertheorie," Hausvogteiplatz 5-7, O-1086 Berlin, Federal Republic of Germany

D. Bimberg
Center for Quantized Electronic Studies, University of California, Santa Barbara, Santa Barbara, California 93106 and Institut für Festkörperphysik, Technische Universität Berlin, Hardenbergstraße 36, W-1000 Berlin 12, Federal Republic of Germany

(Received 16 February 1993)

For spatially indirect excitons in staggered-line-up single quantum wells, binding energies, Bohr radii, and oscillator strengths are calculated, taking into account finite barrier heights and image-charge effects. Numerical results are presented for a model case of particular fundamental importance. For AlAs/GaAs quantum wells, which are indirect in k space, we find binding energies up to 11 meV for the X_z exciton and 5 meV for the X_{xy} exciton. However, no-phonon oscillator strengths fall below the direct exciton by five orders of magnitude. A comparison to experiment suggests that the X_{xy} exciton is lowest in energy.

I. INTRODUCTION

The vast majority of work on fundamental properties of heterostructures and quantum wells (QW's) in the past 20 years has concentrated on nested alignment (type-I) structures.[1] Most details of their electronic and optical properties are well understood. At room temperature, excitons dominate many linear and nonlinear optical properties[1,2] of such QW's due to their strongly enhanced binding energy as compared to three-dimensional materials. Only recently, however, have realistic calculations of binding energies, radii, and oscillator strengths been presented, in which the assumption of infinite barriers was dropped and which took into account properly the effect of image charges[3,4] and valence-band mixing.[5]

Staggered line-up (type-II) heterostructures are as common as type-I structures. The InAs/GaSb structure was among the first whose electronic properties were discussed in great detail.[6,7] Nevertheless only recently was broader attention given to such structures,[8] probably following the observation of their vast potential for devices such as electrically tunable light sources,[9] for example.

The minima of potential energy for electrons and holes do not occur in the same layer for staggered structures, and externally excited charge carriers segregate in adjacent layers. The overlap of the wave functions and the magnitude of the Coulomb interaction are believed to be concomitantly reduced. Following earlier work by Bastard[10] on GaSb/InAs QW's, exciton effects were thus thought to be unimportant in type-II quantum wells. In superlattices with narrow enough barriers the overlap is reestablished and values close to those in type-I systems are predicted.[11] For both uncoupled quantum wells and superlattices, no calculations of binding energies or Bohr radii exist, however, which parallels the work done on excitons in type-I QW's.

It is the purpose of this contribution to present a more accurate theory of type-II excitons in QW's than hitherto available, together with numerical results for the particularly important and experimentally easily accessible[8,12,13] model case AlAs/GaAs. The AlAs/GaAs system is also particularly interesting since the excitons there are additionally indirect in k space, similar to GaP/AlSb or AlSb/AlP.

The X minimum in the AlAs barriers of AlAs/GaAs QW's is below that of GaAs. For well widths below 3.5 nm (Ref. 8) not only the X but also the Γ minimum of GaAs is at higher energy than the AlAs X minimum. Electrons near the X minimum in AlAs exhibit a camel's-back-like dispersion.[14] The related large density of states leads to an appreciable increase of the exciton binding energy. The oscillator strength, on the other hand, will be low in single quantum wells due to the indirect character of the transition. Recently[12] results of luminescence experiments for such single QW's were presented and will be discussed here in detail.

II. CALCULATION OF EXCITON BINDING ENERGY

We start with the derivation of exciton properties for the more complex situation of the k indirect case. The effective-mass equation for the exciton at one X minimum is given by

$$\left[-\frac{\hbar^2}{2m_{e\|}}\partial_{z_e}^2-\frac{\hbar^2}{2m_{h\|}}\partial_{z_h}^2-\frac{\hbar^2}{2\mu_\perp}\Delta_\rho+V_e(z_e)+V_h(z_h)\right.$$

$$\left.+V_x(\rho,z_e-z_h)\right]\Phi(\mathbf{r}_e,\mathbf{r}_h)=\mathcal{E}_x\,\Phi(\mathbf{r}_e,\mathbf{r}_h)\ , \quad (1)$$

where $\boldsymbol{\rho}=\boldsymbol{\rho}_e-\boldsymbol{\rho}_h$ is the relative motion within the quantum-well plane (z is directed along the growth axis). The masses ($\|$ for the growth direction, $\perp$ for the QW

plane) have to be chosen according to the band-structure minimum under consideration (see below).

As long as we neglect the difference in the dielectric constants (DC) for well and barrier, the Coulomb potential forming the exciton is

$$V_x(\rho,z) = -\frac{e^2}{\epsilon\sqrt{\rho^2+z^2}} \ . \tag{2}$$

The total electron-hole wave function Φ is separated into the motion of electron and hole along z and the in-plane motion of the exciton $\phi(\rho)$,

$$\Phi(\mathbf{r}_e,\mathbf{r}_h) = u_e(z_e)\,u_h(z_h)\,\phi(|\,\boldsymbol{\rho}_e - \boldsymbol{\rho}_h\,|) \ . \tag{3}$$

The hole is properly localized in the GaAs well, and we can use for $u_h(z_h)$ the confinement function of the first heavy-hole sublevel. In contrast, the X electron is found in the AlAs material and bound by Coulombic forces only. The proper determination of its wave function $u_e(z_e)$ is the main issue of the present section. Bastard[10] used a variational calculation in the type-II system $In_xGa_{1-x}As/GaSb$. The AlAs/GaAs system has been recently treated variationally by Duggan.[11] Additionally, a deformation of the hole wave function by the Coulomb attraction of the electron has been included, but the penetration of both wave functions into the adjacent material was neglected. A problem with some similarities to the staggered excitons deals with type-I QW's having a valence-band offset near to zero, as for $Cd_xMn_{1-x}Te/CdTe$. The variational approach[15] was improved by a full numerical solution of the hole confinement by Wu.[16] We follow this method by averaging with the yet unknown exciton wave function and solve the resulting Schrödinger equation for $u_e(z_e)$ numerically,

$$\left[-\frac{\hbar^2}{2m_{e\|}}\partial_{z_e}^2 + V_e(z_e) + W_x(z_e) + K_x + E_h - \mathcal{E}_x\right] u_e(z_e) = 0 \ . \tag{4}$$

Here,

$$K_x = \frac{\hbar^2}{2\mu_\perp}\int_0^\infty d\rho\,\rho\,[\partial_\rho\phi(\rho)]^2 \tag{5}$$

is the kinetic energy of the exciton, and the effective electron potential W_x,

$$W_x(z_e) = \int_{-\infty}^{+\infty} dz_h u_h^2(z_h)\int_0^\infty d\rho\,\rho\,\phi^2(\rho)\,V_x(\rho,z_e-z_h) \ , \tag{6}$$

is superimposed to the repulsive step potential $V_e(z_e) = \Delta_X^e\Theta(|z_e| - L/2)$. The difference in the dielectric constants between GaAs ($\epsilon_W = 12.53$) and AlAs ($\epsilon_B = 10.06$) is large enough to make image potentials important,[3,4] thus extending the theory of Ref. 16. The dominant interaction is of cross character (electron in AlAs, hole in GaAs), for which the modified Coulomb potential reads

$$V_x(\rho,z) = -\frac{2e^2}{(\epsilon_W+\epsilon_B)}\sum_{k=0,1,\ldots}^{\infty}\frac{Q^k}{\sqrt{\rho^2+(z+kL)^2}} \tag{7}$$

with the dielectric misfit

$$Q = \frac{\epsilon^W - \epsilon^B}{\epsilon^W + \epsilon^B} \ . \tag{8}$$

For AlAs/GaAs, $Q = 0.11$ which gives roughly the relative correction expected for the exciton binding energy. The prefactor in (7) resembles the arithmetic mean of well and barrier DC. However, for the small well widths of interest here, the total expression is closer to the barrier value.

To simplify the calculation we have used for the in-plane motion of the exciton the ansatz

$$\phi(\rho) = \frac{2}{a_x}e^{-\rho/a_x} \tag{9}$$

and minimized the resulting eigenvalue $\mathcal{E}_x$ from (4) with respect to the two-dimensional exciton radius a_x. A close inspection of the potential $W_x(z_e)$ shows that it behaves as $-e^2/(\epsilon_B z_e)$ at large distances but reaches a finite value at zero distance. Together with the repulsive term $V_e(z_e)$ it forms a double well outside both interfaces where the electron can be bound. The resulting exciton binding energy is given by $E_B = E_h - \mathcal{E}_x$. The band-edge energies for both materials are taken from Ref. 17. Using a 70% conduction-band offset the confining potentials can be derived as $\Delta_\Gamma^e = 1068$ meV, $\Delta_X^e = -197$ meV, and $\Delta_\Gamma^h = 457$ meV. For the indirect Γ-X transition, an incomplete confinement of the electron in AlAs and the hole in GaAs results. Therefore, the assumption of infinite barrier height[10] is not justified here.

III. RESULTS AND DISCUSSION

In the numerical calculations, we have used a well width of $L = 2$ nm in accordance with the available experimental data.[12] The electron and hole wave functions are shown in Fig. 1. Apart from the electron wave function with even parity shown in Fig. 1, there is an odd state only 0.2 meV above with—apart from a sign—nearly the same wave function. Thus, thinking of the electron as localized either at the left or at the right interface is fairly correct.

Another lifted degeneracy is related to the inequivalent role of the X minima. The question of which of the AlAs X states are lowest in energy has been discussed in the literature controversially for quite a while. Recent optically detected magnetic resonance experiments on superlattices[18] seem to indicate that for an AlAs barrier thickness larger than 5.5 nm the in-plane oriented minima (X_{xy} states) become lowest due to strain, whereas for smaller barrier widths the X_z states are at lower energy. Our experimental results discussed below indeed show that for our barrier width of 18 nm the X_{xy} exciton is at lowest energy.

The conduction-band minimum in AlAs is slightly displaced from the X point, and the dispersion exhibits a

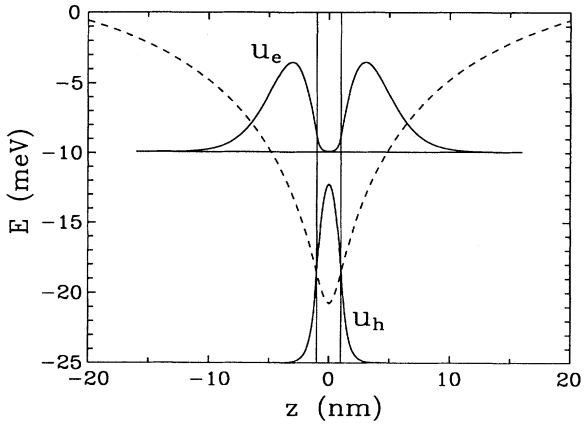

FIG. 1. Indirect type-II exciton in an $L = 2$ nm AlAs/GaAs quantum well marked by vertical lines. Dashed curve, effective potential of the X electron due to the Coulomb attraction by the hole. u_e and u_h, wave function of the X electron and the Γ hole, respectively.

very flat shape there (energy difference only 0.2 meV between X point and minimum[17]). To account for this camel's-back structure[14] at least approximately, we have calculated the (anisotropic) X exciton in AlAs bulk material using an effective longitudinal electron mass. In order to get the binding energy of $E_{B,\mathrm{bulk}} = 25.9$ meV,[14] we have to adopt the large value of $m_{eX,l} = 4.1 m_0$. For the type-II quantum well, the electron in an X_z valley then comes close to the interface and gains much Coulomb energy. The four X_{xy} valleys exhibit a much smaller mass along z, $m_{eX,tr} = 0.19 m_0$, and less confinement is possible. The in-plane mass relevant for the kinetic energy of the exciton scales in the other direction but cannot outweigh the z effect, and we found the X_z exciton binding energy to be always the larger one. For $L = 2$ nm we obtained an X_z binding energy of 9.9 meV and an exciton radius of 9.7 nm. The corresponding X_{xy} exciton values are $E_B = 4.1$ meV and $a_x = 15.0$ nm, respectively.

To have a general impression of the dependence on well width we display in Fig. 2 calculated binding energies for both indirect excitons and compare these with the direct exciton at the Γ point, again calculated with image charge effects.[4] As expected, the direct exciton has a much larger binding energy since hole and electron are both confined in the well. But note that due to the strong confinement of the Γ electron, the direct exciton is higher in absolute energy for well widths below 3.5 nm (direct-indirect crossover). At $L = 2$ nm, the direct exciton is 168 meV above the X_{xy} exciton.

For the direct exciton, the variational determination of the exciton radius has been checked against a full solution of the in-plane Schrödinger equation, shown as dots in Fig. 2. The difference is small enough to trust the variational procedure. The corresponding exciton radii are shown in Fig. 3.

A short remark concerns the influence of interface-roughness-induced well-width fluctuations on the exciton line shape. The difference in radii between direct and indirect exciton is not the decisive factor. Much more

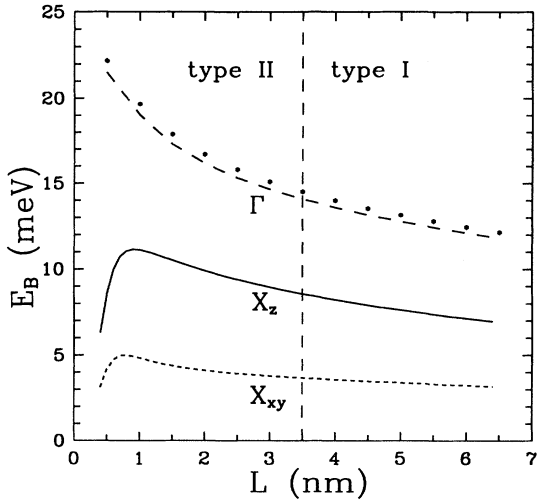

FIG. 2. Exciton binding energies E_B in AlAs/GaAs quantum wells in dependence on well thickness L. Γ, direct exciton at the Γ point (dots are the numerical solution of the in-plane exciton equation); X_z and X_{xy}, indirect excitons at the X point.

important is the well-width dependence of the absolute exciton energy. Let us compare the exciton energies in islands with seven and eight monolayers thickness ($L = 1.98$ nm and 2.26 nm, respectively). The energy difference amounts to 64.1 meV for the direct exciton and 16.3 meV at the indirect one since for the latter only the hole confinement contributes. As a result, the indirect exciton is expected to have the smaller linewidth.

The optical transition matrix element without phonons is given by (photon wave vector negligible)

$$M_X = \left| \phi^X(0) \frac{1}{A} \int d\mathbf{r}\, u_e^X(z)\, u_h^\Gamma(z)\, e^{i\mathbf{Q}\cdot\mathbf{r}} \right|^2 , \qquad (10)$$

where $\mathbf{Q}$ is the momentum difference between the Γ point and one of the X points in reciprocal space. The un-

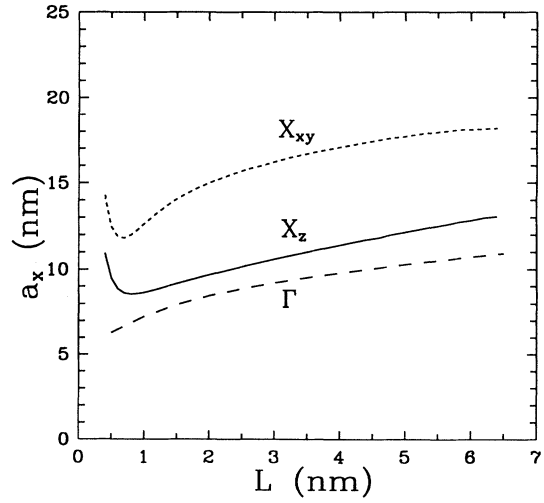

FIG. 3. Variational in-plane exciton radii a_x corresponding to Fig. 2.

derlying conduction-band Bloch functions have been approximated by the phase factor containing $\mathbf{Q}$ (see the discussion below). The integration in (10) extends over the normalization area A in the quantum-well plane and all z values.

If $\mathbf{Q}$ is directed along the growth direction (X_z valley), a finite result is obtained in agreement with the calculation by Pulsford.[19] Thus, a nonvanishing no-phonon (NP) line is expected both for superlattices and single QW's. However, the numerical value of the NP matrix element is extremely small. For $L = 2$ nm, which is only four times the lattice constant, we obtained 1.2×10^{-5} of the direct Γ-exciton value being given as

$$M_\Gamma = \left| \phi^\Gamma(0) \frac{1}{A} \int d\mathbf{r}\, u_e^\Gamma(z) u_h^\Gamma(z) \right|^2 . \tag{11}$$

The lifetime of X_z excitons is thus expected to be in the 30-μs range, scaling the known lifetime of the direct exciton [0.3 ns in $Al_{0.4}Ga_{0.6}As/GaAs$ quantum wells with $L_z = 2$ nm (Ref. 20)]. This rather long lifetime is in agreement with experimental values by Wilson[8] and Finkman.[21]

To be more precise, M_{Xz} gets a finite value since the confinement potential in the z direction mixes the Γ- and X-like wave functions, thus breaking the bulk selection rule. The magnitude of M_{Xz} and thus the intensity of the NP line is expected to decrease with increasing difference between the Γ and X conduction-band states in agreement with experimental observations on structures where the X_z exciton has the lowest energy.[8,11,13]

Turning to the X_{xy} exciton, the NP transition has zero probability since the center-of-mass momentum of the exciton in the layer plane persists as a good quantum number. This can be seen from Eq. (10), where the phase factor $\exp(iQ_x x)$ integrates to zero.

Figure 4 compares the low-temperature luminescence spectra[12] of a 2-nm AlAs/GaAs QW in two different samples. Both samples were grown under identical conditions with the exception that in one sample the growth was interrupted for 100 s at both interfaces, whereas the other one was grown without interruption. First, it is absolutely striking how weak the no-phonon transition is. In samples with only slightly coupled wells[8,11,13,18] where the X_z exciton is lowest in energy, the intensity of the NP line is typically an order of magnitude larger than

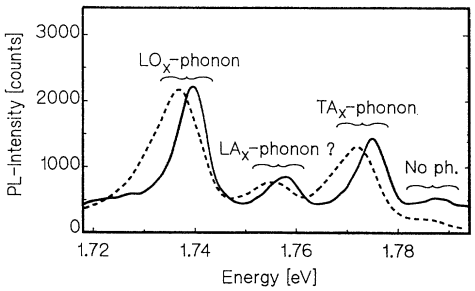

FIG. 4. Low-temperature photoluminescence spectra of AlAs/GaAs quantum wells without (full curve) and with a 100-s growth interruption (dashed curve). Well width 2 nm, excitation level 50 W/cm^2.

the intensity of the momentum-conserving (MC) phonon replica. Second, the NP line completely vanishes in the growth-interrupted sample which has interfaces of much higher perfection.[12] Here, the intensity of the NP line depends solely on the mixing of the X_{xy} states with the Γ states which can be induced by potential fluctuations associated with interface roughness. Both observations exclude the assignment of the luminescence in Fig. 4 to the X_z exciton.

We add a preliminary consideration concerning the phonon-assisted transitions. They can be calculated using first-order perturbation theory with respect to the electron–LO-phonon coupling (Fröhlich interaction). Physically, the indirect X exciton (initial state) emits a phonon using the direct exciton as an intermediate state, and decays finally into a photon. One might expect that the electron-phonon coupling is enhanced by the charge separation in real space since the phonon emission is driven by the charge distribution of the X exciton. For the X_z exciton, we have apart from an energy denominator

$$M_{\text{phonon}} = (\epsilon_\infty^{-1} - \epsilon_S^{-1}) \left| \int d\boldsymbol{\rho}\, \phi^X(\rho)\, \phi^\Gamma(\rho) \right|^2 \times \int_{-\infty}^{+\infty} dz\, |A(z)|^2 , \tag{12}$$

where the charge distribution integrated along z enters

$$A(z) = \int_{-\infty}^{z} dz' \left[u_e^\Gamma(z')\, u_e^X(z')\, e^{iQz'} - (u_h^\Gamma(z'))^2\, W \right] \tag{13}$$

with $W = \int_{-\infty}^{+\infty} dz' u_e^\Gamma(z')\, u_e^X(z') \exp(iQz')$. Contrary to the expectation, the matrix element remains rather small due to the doubly indirect nature of the integrand — small overlap between electron and hole wave function and rapidly oscillating factors. A closer inspection of the phonon-assisted transition probabilities in quantum wells is deferred to a forthcoming publication.

IV. CONCLUSION

An improved theory of excitons in staggered line-up (type-II) quantum wells is presented and realistic binding energies and oscillator strengths for X_z and X_{xy} excitons are calculated for AlAs/GaAs QW's, which serves as a model system for two-dimensional excitons being indirect in real as well as momentum space. Surprisingly large binding energies result. The low oscillator strengths observed here are caused by the indirect transition in k space. We expect for k space direct type-II transition oscillator strengths which are not much less than those in type-I systems explaining the strong interface luminescence recently reported for the type-II $In_xAl_{1-x}As/InP$ structure.[22]

ACKNOWLEDGMENTS

Part of this work was performed in the framework of SFB 6 of the Deutsche Forschungsgemeinschaft. D.B. is very grateful for the hospitality of J.L. Merz at QUEST.

[1]R. Dingle, in *Semiconductors and Semimetals,* edited by R.K. Willardson and A.C. Beer (Academic, San Diego, 1987), Vol. 24; C. Weisbuch and B. Vinter, *Quantum Semiconductor Structures* (Academic, San Diego, 1991).
[2]J. Christen and D. Bimberg, Phys. Rev. B **42**, 7213 (1990).
[3]L.V. Keldysh, Superlatt. Microstruct. **4**, 637 (1988).
[4]D.B. Tran Thoai, R. Zimmermann, M. Grundmann, and D. Bimberg, Phys. Rev. B **42**, 5906 (1990).
[5]G.D. Sanders and Y.C. Chang, Phys. Rev. B **35**, 1300 (1987).
[6]G.A. Sai-Halasz, L. Esaki, and W.A. Harrison, Phys. Rev. B **18**, 2812 (1978).
[7]P. Voisin, G. Bastard, and C.E.T. Gonzalves da Silva, Solid State Commun. **39**, 79 (1981).
[8]See the review by B.A. Wilson, IEEE J. Quantum Electron. **24**, 1763 (1988).
[9]H. Kroemer and G. Griffiths, IEEE Electron Dev. Lett. **ED-L4**, 20 (1983); E.J. Caine, S. Subbanna, H. Kroemer, and J. Merz, Appl. Phys. Lett. **45**, 1123 (1984).
[10]G. Bastard, Phys. Rev. B **24**, 4714 (1981); *Wave Mechanics Applied to Semiconductor Heterostructures* (Les Editions de Physique, Les Ulis, 1988), p. 139.
[11]G. Duggan and H.I. Ralph, Proc. SPIE **792**, 147 (1987).
[12]D. Bimberg, F. Heinrichsdorff, R.K. Bauer, D. Gerthsen, D. Stenkamp, D.E. Mars, and J.N. Miller, J. Vac. Sci. Technol. B **10**, 1793 (1992).
[13]J. Feldmann, J. Nunnenkamp, G. Peter, E. Goebel, J. Kuhl, K. Ploog, P. Dawson, and C.T. Foxon, Phys. Rev. B **42**, 5809 (1990).
[14]D. Bimberg, W. Bludau, R. Linnebach, and E. Bauser, Solid State Commun. **37**, 987 (1981).
[15]S.K. Chang, A.V. Nurmikko, J.W. Wu, L.A. Kolodziejski, and R.L. Gunshor, Phys. Rev. B **37**, 1191 (1988).
[16]Ji-Wei Wu, Solid State Commun. **67**, 911 (1988).
[17]*Landolt-Börnstein, New Series*, Group III, Vol. 17, Pt. a, edited by O. Madelung, M. Schulz, and H. Weiss (Springer, Berlin, 1982).
[18]H.W. van Kesteren, E.C. Cosman, P. Dawson, K.J. Moore, and C.T. Foxon, Phys. Rev. B **39**, 13 426 (1989).
[19]N.J. Pulsford, R.J. Nicholas, P. Dawson, K.J. Moore, G. Duggan, and C.T. Foxon, Phys. Rev. Lett. **63**, 2284 (1989).
[20]J. Christen, D. Bimberg, G. Weimann, and G. Schlapp, Appl. Phys. Lett. **44**, 84 (1984).
[21]E. Finkman, M.D. Sturge, and M.C. Tamargo, Appl. Phys. Lett. **49**, 1299 (1986).
[22]J. Böhrer, T. Wolf, A. Krost, and D. Bimberg, Phys. Rev. B **47**, 6439 (1993).